Diminishing Dynamic Motion Problems of Platinum Anticancer Drug Adducts of Guanine Derivatives with the Hybrid Ligand Approach: Evidence for Cis Interligand Interactions Especially between 3′-GMP's

Hing C. Wong,[†] Francesco P. Intini,[‡] Giovanni Natile,*[,‡] and Luigi G. Marzilli*[,†]

Department of Chemistry, Emory University, Atlanta, Georgia 30322, and Dipartimento Farmaco-Chimico, Università degli Studi di Bari, 70125 Bari, Italy

Received October 9, 1998

The key problem obscuring the role of the ammine and primary amine groups in the activity of clinically used Pt anticancer drugs is the dynamic character of adducts with DNA and DNA constituents. To address this problem, we introduced the hybrid ligand approach with the diamine **pipen** = 2-(aminomethyl)piperidine; the piperidine ring greatly reduces dynamic motion in adducts. We now use NMR and CD methods to investigate (*S,R*)- and (*R,S*)-**pipen**Pt**G**$_2$ complexes (with *S,R* and *R,S* configurations at the N and C **pipen** asymmetric centers, respectively; **G** = a guanine derivative). Each **pipen**Pt**G**$_2$ complex can have two head-to-head (HH) and two head-to-tail (HT) rotamers. However, only the two HT atropisomers were detected. The Δ or Λ chirality of each HT rotamer was determined from NOESY/EXSY spectra and/or the sign of the CD signal. Examination of adducts with **G** = 5′-GMP, 3′-GMP, or 9-EtG (9-ethylguanine) allowed us to assess the effects of different N9 substituents and **pipen** chirality on the stability and spectral properties of the atropisomers. For the 9-EtG complexes, the HT atropisomers were nearly equally stable, indicating that the **pipen** configuration has little influence when the N9 substituent lacks a phosphate group. However, for GMP complexes, several factors influence both relative abundance and shifts of the H8 signals of the ΔHT and ΛHT forms at neutral pH. The chirality of the major HT form of the (*S,R*)- and (*R,S*)-**pipen**Pt(5′-GMP)$_2$ complexes was Λ and Δ, respectively. Therefore, the chirality of the **pipen** ligand is an important determinant of HT chirality for **pipen**Pt(5′-GMP)$_2$. Since, for 5′-GMP, phosphate−NH-(**pipen**) hydrogen bonding is possible, this interaction probably favors the major atropisomer, in which two such interactions are possible, over the minor atropisomer, in which only one interaction is possible. The ΔHT form was dominant for *both* (*S,R*)- and (*R,S*)-**pipen**Pt(3′-GMP)$_2$. The stability arises from the more favorable interactions between the phosphates and the NH's of the cis 3′-GMP's in the ΔHT vs the ΛHT form. This hydrogen bonding is more favorable when the **G** bases have less tilt, and less tilted **G**'s are associated with more favorable dipole−dipole interactions and deshielded H8 signals. We showed that 3′-GMP adducts favor the ΔHT conformer at pH7; the ΔHT conformer preference explains the enhanced "Δ" CD signal observed for most 3′-GMP adducts, including the cisplatin adduct.

Introduction

Although the discovery of the anticancer activity of *cis*-$PtCl_2(NH_3)_2$ (cisplatin) has prompted much research, the mechanism of action of this Pt drug and its analogues, *cis*-PtA_2X_2 (A_2 is two amines or a bidentate amine ligand, and X is a leaving group), is still not clear, but DNA appears to be the principal target.[1] One of the early structure−activity relationships developed indicated that at least one amine proton must be present in the carrier A_2 ligand in order to maintain anticancer activity. This observation has led to the hypothesis that O6−NH[2−10] and/or phosphate−NH[3−16] intramolecular hydrogen bonding within the Pt−DNA adduct influences structure and hence activity. A serious limitation in studies of adducts between Pt anticancer drugs and DNA, including DNA constituents from simple nucleobases through oligonucleotide adducts, is the fluxional character of these adducts. We have called this limitation the "dynamic motion problem" and recently described its consequences.[17]

To investigate which types of hydrogen bonding are possible

[†] Emory University.
[‡] Università degli Studi di Bari.

(1) Reedijk, J. *Chem. Commun.* **1996**, 801.
(2) Xu, Y.; Natile, G.; Intini, F. P.; Marzilli, L. G. *J. Am. Chem. Soc.* **1990**, *112*, 8177.
(3) Kiser, D.; Intini, F. P.; Xu, Y.; Natile, G.; Marzilli, L. G. *Inorg. Chem.* **1994**, *33*, 4149.
(4) Hambley, T. W. *Inorg. Chem.* **1991**, *30*, 937.
(5) Ling, E. C. H.; Allen, G. W.; Hambley, T. W. *J. Am. Chem. Soc.* **1994**, *116*, 2673.
(6) Vickery, K.; Bonin, A. M.; Fenton, R. R.; O'Mara, S.; Russell, P. J.; Webster, L. K.; Hambley, T. W. *J. Med. Chem.* **1993**, *36*, 3663.
(7) Fenton, R. R.; Easdale, W. J.; Er, H. M.; O'Mara, S. M.; McKeage, M. J.; Russell, P. J.; Hambley, T. W. *J. Med. Chem.* **1997**, *40*, 1090.
(8) Rezler, E. M.; Fenton, R. R.; Easdale, W. J.; McKeage, M. J.; Russell, P. J.; Hambley, T. W. *J. Med. Chem.* **1997**, *40*, 3508.
(9) Hambley, T. W. *Coord. Chem. Rev.* **1997**, *166*, 181.
(10) Guo, Z.; Sadler, P. J.; Zang, E. *J. Chem. Soc., Chem. Commun.* **1997**, 27.
(11) Berners-Price, S. J.; Frey, U.; Ranford, J. D.; Sadler, P. J. *J. Am. Chem. Soc.* **1993**, *115*, 8649.
(12) Berners-Price, S. J.; Ranford, J. D.; Sadler, P. J. *Inorg. Chem.* **1994**, *33*, 5842.
(13) Berners-Price, S. J.; Frenkiel, T. A.; Ranford, J. D.; Sadler, P. J. *J. Chem. Soc., Dalton Trans.* **1992**, 2137.
(14) Bloemink, M. J.; Heetebrij, R. J.; Inagaki, K.; Kidani, Y.; Reedijk, J. *Inorg. Chem.* **1992**, *31*, 4656.
(15) Reedijk, J. *Inorg. Chim. Acta* **1992**, *198−200*, 873.
(16) Fouts, C. S.; Marzilli, L. G.; Byrd, R. A.; Summers, M. F.; Zon, G.; Shinozuka, K. *Inorg. Chem.* **1988**, *27*, 366.

10.1021/ic981198f CCC: $18.00
Published on Web 02/19/1999

Chart 1. 5′-GMP Structure and Numbering Scheme[a]

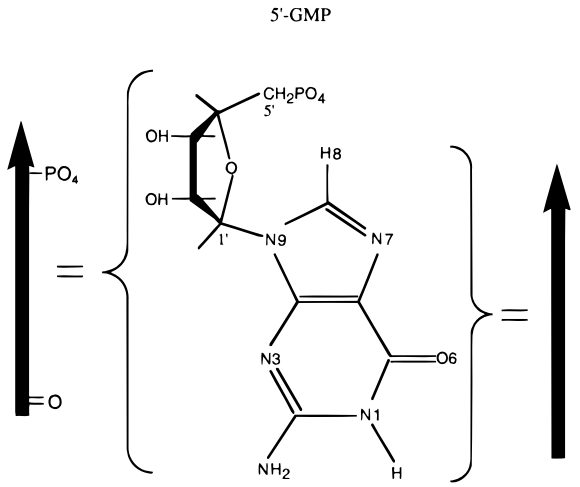

[a] The arrow on the right defines the base directional properties (see the caption to Figure 1). The arrow on the left is used to depict hydrogen-bonding motifs involving the phosphate group or O6 of 5′-GMP.

and could play a role in stabilizing the structure of DNA adducts, we have been evaluating *cis*-PtA_2**G**$_2$ model complexes, in which A_2 is a bulky bidentate amine ligand and **G** is a unidentate guanine derivative (Chart 1).[2,3,17−19] We are exploring how the specific orientation of NH groups influences the atropisomers of such *cis*-PtA_2**G**$_2$ complexes. The **G** bases can be oriented in a head-to-head (HH) or a head-to-tail (HT) arrangement (Figure 1). There are two possible HT orientations, which differ in chirality and are designated ΛHT and ΔHT (Figure 1).[17] The symmetry of the *cis*-PtA_2**G**$_2$ complex influences the number of atropisomers. For non-C_2-symmetrical A_2 ligands, two HH and two HT atropisomers are possible. With a bulky A_2 carrier ligand, interconversion between atropisomers by rotation around the Pt−N7 bonds is slow on the NMR time scale.[20] Different atropisomers can be detected by the number of observed H8 NMR signals.[2,3,18,19]

Our studies with *cis*-PtA_2**G**$_2$ complexes of the C_2-symmetrical carrier ligands **Me$_2$DAB** (*N*,*N*′-dimethyl-2,3-diaminobutane)[2,19] and **Bip** (2,2′-bipiperidine)[18] (Figure 2) demonstrated that the configuration of the secondary NH's strongly influenced the ΛHT/ΔHT atropisomer ratio such that one or the other HT form was highly favored. Since the nature of the **G** N9 substituent has only a secondary modulating effect, we have called these C_2-symmetrical ligands chirality-controlling chelate (**CCC**) ligands.[18,19,21]

(**CCC**)Pt**G**$_2$ complexes with **Me$_2$DAB** and **Bip** carrier **CCC** ligands having the same chirality, e.g. the *S*,*R*,*R*,*S* configurations of the four asymmetric centers (N, C, C, and N) in the chelate ring, and the same **G** derivative have very similar equilibrium atropisomer distributions, chemical shifts, etc. The dynamic properties, however, are very different. The **Bip** derivatives atropisomerize very slowly, allowing us to determine the initial distribution of rotamers during the attack of the **G** ligands on Pt.[18] In contrast, the **Me$_2$DAB** complexes have greater fluxionality, more similar to such behavior in complexes with clinically used carrier ligands. The secondary amine center can isomerize at neutral pH in the **Me$_2$DAB** but not in the **Bip** complexes. Larger nucleic acid constituent adducts are now being studied with complexes of the **Bip** ligand. These provide a powerful solution to the dynamic motion problem, and their study is proving to be rewarding. However, the environment of both coordinated nucleobases is very different from that provided by anticancer drugs.

More recently, we began to address the dynamic motion problem by studying complexes with 2-(aminomethyl)piperidine (**pipen**) (Figure 3), a hybrid between the **CCC** type of ligand and a nonbulky ligand. This ligand contains a secondary amine enclosed within a piperidine (pip) ring, which reduces dynamic motion significantly, and a primary amine that could allow some flexibility. The hybrid nature of the **pipen** ligand allowed us to evaluate interactions of the **G** derivative with a cis primary amine. This **G** is within an environment similar to that for the anticancer drugs, which are generally more active with primary

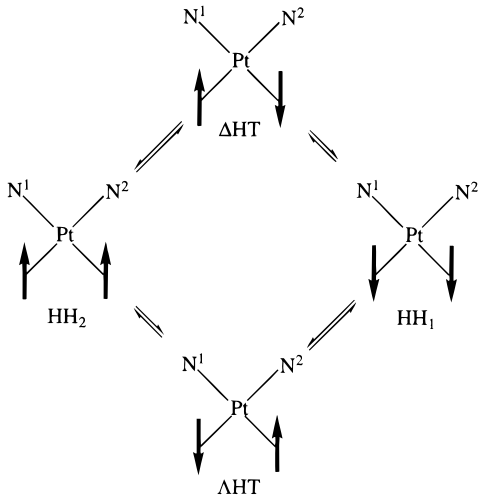

Figure 1. Shorthand representation of ΛHT, ΔHT, and HH conformations with the carrier ligand to the rear. When the carrier is C_2-symmetric and N^1 equals N^2, the two HH forms shown are identical. Arrows represent the **G** bases with **G** H8 near the tip and with the **G** O6 near the blunt end and projecting toward the carrier. The **G** O6's are used to define HT chirality. When the complexes are viewed from the **G** side of the coordination plane, a line connecting the O6 atoms will be rotated (by an angle < 90°) clockwise (ΛHT) or counterclockwise (ΔHT) in order to be aligned with the perpendicular to the coordination plane. For the (*S*,*R*)-**pipen**Pt**G**$_2$ complexes, N^2 and N^1 represent the primary and the secondary amine nitrogens, respectively, and all four (ΛHT, ΔHT, and the two HH) conformations shown are theoretically possible.

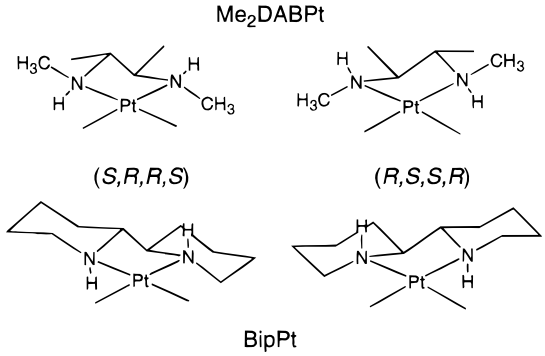

Figure 2. Sketches of **Me$_2$DAB**Pt and **Bip**Pt with *S*,*R*,*R*,*S* and *R*,*S*,*S*,*R* configurations.

(17) Wong, H. C.; Coogan, R.; Intini, F. P.; Natile, G.; Marzilli, L. G. *Inorg. Chem.* **1999**, *38*, 777.
(18) Ano, S. O.; Intini, F. P.; Natile, G.; Marzilli, L. G. *J. Am. Chem. Soc.* **1997**, *119*, 8570.
(19) Marzilli, L. G.; Kiser, D.; Wong, H. C.; Ano, S. O.; Marzilli, P. A.; Intini, F. P.; Natile, G. *Inorg. Chem.* **1998**, *37*, 6898.
(20) Cramer, R. E.; Dahlstrom, P. L. *J. Am. Chem. Soc.* **1979**, *101*, 3679.
(21) Ano, S. O.; Intini, F. P.; Natile, G.; Marzilli, L. G. *Inorg. Chem.*, submitted for publication.

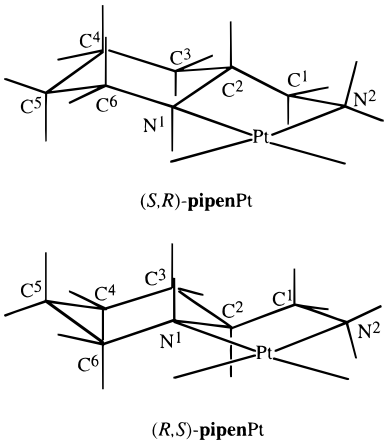

Figure 3. Numbering scheme for the (*S*,*R*)- and (*R*,*S*)-**pipen**Pt ligands.

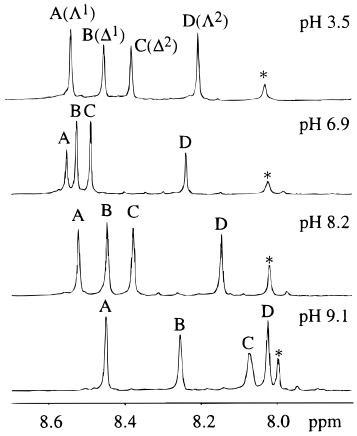

Figure 4. H8 regions of the ^{1}H NMR spectra of (*S*,*R*)-**pipen**Pt(3′-GMP)$_2$ at various pH values. Δ and Λ indicate the chiralities of the HT atropisomer, and the superscripts 1 and 2 denote the coordination sites cis to the secondary and the primary amine, respectively. The peaks labeled with an asterisk are from free 3′-GMP.

than with secondary amine carrier ligands. In fact, platinum complexes containing the **pipen** ligand do show anticancer activity.[22,23]

In a study of (*S*,*R*)-**pipen**Pt(5′-GMP)$_2$,[17] the observation at pH 3 of only four major H8 NMR signals in two sets and the absence of any H8−H8 NOE/EXSY cross-peaks indicated the dominance of the two HT atropisomers in a 2:1 ratio. Neither of the two possible HH atropisomers was detected. Such results suggested that several factors other than NH hydrogen bonding may contribute to the relative stability of the atropisomers and that the more favorable base−base dipole interactions are responsible for the dominance of the HT forms. Since the previous study was limited in scope, we have now employed both NMR and CD (circular dichroism) spectroscopies to study (*S*,*R*)- and (*R*,*S*)-**pipen**Pt**G**$_2$ complexes with **G** = 3′-GMP, 5′-GMP, and 9-ethylguanine (9-EtG). Different **G** moieties were chosen in order to investigate the effect on the conformational equilibrium of the presence of a phosphate group, the position of that phosphate group, and the absence of a sugar−phosphate group.

Finally, about two decades ago, we observed that simple *cis*-PtA$_2$(GMP)$_2$ complexes had enhanced CD signals[24] in similar spectral regions where the CD signal of DNA was enhanced by binding of anticancer drugs.[25,26] This unusual observation was difficult to explain in view of the dynamic motion problem, which prevented NMR characterization of solution conformers. The studies described herein contribute to our understanding of the origins of the enhanced CD signals.

Experimental Section

Preparation of pipenPtG$_2$ Solutions. Twenty millimolar solutions of the **G**'s (Sigma, used as received) in D_2O (0.6 mL) were prepared, and the pH was adjusted to ∼3.5 by careful addition of deuterated nitric acid. A lower pH (∼1.6) was required to dissolve 9-EtG. PtCl$_2$(**pipen**) (0.5 equiv) was then added, the pH values of the reaction mixtures were adjusted back to ∼3.5, and the solutions were stirred at 50 °C for 3 days. The pH (uncorrected) of samples in NMR tubes was adjusted with 1% and 10% (w/v) D_2O solutions of DNO_3 or NaOD. NaCl was added to samples for pH titration experiments to give an ionic strength of 0.1 M.

NMR Spectroscopy. ^{1}H NMR 1D spectra were obtained with either a GE GN 500 MHz or a GE Omega 600 MHz spectrometer. For pH titration experiments, sodium 3-(trimethylsilyl)propionate-d_4 (TSP) was used as an external reference; otherwise, all spectra were referenced to the HOD peak. 2D phase-sensitive chemical exchange correlation spectra, NOESY/EXSY[27] (one K × 2K matrix with a mixing time of 300 ms; 32 acquisitions per t_1 period), were obtained at 5 °C on the 600 MHz spectrometer with a spectral window in both dimensions of 6250 Hz. Spectra were processed with the FELIX program (Molecular Simulations, Inc.). An exponential multiplication function with a line broadening of 1 Hz was applied in the acquisition dimension, and the baseline was corrected using a polynomial function of zero order. The evolution dimension was zero-filled to 2K points, and a 90° shifted skewed sine squared function was applied.

CD Spectroscopy. CD spectra of ∼4 × 10^{-5} M solutions were recorded on a JASCO 600 spectropolarimeter at ambient temperature. To improve the signal/noise ratio, four spectra were acquired in succession and averaged.

Results

NMR Results. In the 2D NOESY/EXSY spectra of (*S*,*R*)- and (*R*,*S*)-**pipen**Pt(3′-GMP)$_2$ complexes, there were no cross-peaks between the four H8 signals in each spectrum. This absence of cross-peaks (Supporting Information) suggests that the H8's are remote, consistent with HT atropisomers lacking H8−H8 NOE cross-peaks. Importantly, there were no EXSY cross-peaks between the H8 signals, indicating that the rate of atropisomerization between the HT rotamers is slow on the NMR time scale.

***(S,R)*-pipenPt(3′-GMP)$_2$.** In the ^{1}H NMR spectrum of (*S*,*R*)-**pipen**Pt(3′-GMP)$_2$ at pH 3.5 (Figure 4), the relatively downfield shift of the 3′-GMP H8 signals (8.6−8.1 ppm, labeled A to D) compared to that for free 3′-GMP and the acidic pH used for sample preparation indicates that 3′-GMP is coordinated via N7. By integration, the areas of peaks A and D are equivalent and the areas of peaks B and C are equivalent. The ratio of the sum of the areas of A and D to that of B and C is 1.3:1. Therefore, the major atropisomer at this pH, with peaks A and D, is only slightly more abundant than the minor atropisomer. The 6.1−5.6 ppm region contains five NH signals, which have cross-peaks to the **pipen** methylene and the methine signals in the 3.1−1.0 ppm region. The NH to ND exchange is very slow at low pH.

(22) Morikawa, K.; Honda, M.; Endoh, K.-I.; Matsumoto, T.; Akamatsu, K.-I.; Mitsui, H.; Koizumi, M. *J. Pharm. Sci.* **1990**, *79*, 750.
(23) Tanabe Seiyaku Co., Ltd. Jpn. Kokai Tokkyo Koho JP 59 67,262, 1984.
(24) Marzilli, L. G.; Chalilpoyil, P. *J. Am. Chem. Soc.* **1980**, *102*, 873.
(25) Srivastava, R. C.; Froehlich, J.; Eichhorn, G. L. *Biochimie* **1978**, *60*, 879.
(26) Macquet, J.-P.; Butour, J.-L. *Eur. J. Biochem.* **1978**, *83*, 375.
(27) Kumar, A.; Ernst, R. R.; Wüthrich, K. *Biochem. Biophys. Res. Commun.* **1980**, *95*, 1.

Table 1. Chemical Shifts (ppm) of the Four Major H8 Signals of **pipen**Pt(3′-GMP)$_2$ at pH 3.5 and Their Cross-Peaks with the NH and C^{6}H Signals (H1′ Chemical Shifts Also Included)

	H8	NH[a]	C^{6}H′	C^{6}H″	vol ratio[b]	H1′
		(*S*,*R*)-**pipen**Pt(3′-GMP)$_2$				
A (Λ^1)[c]	8.53	N^{1}H: 6.06 (3.5)	2.42 (7.1)	2.72 (1.0)	0.3	5.92
B (Δ^1)	8.45	N^{1}H: 5.71 (0.6)	2.60 (10.9)	2.88 (10.9)	18.2	5.89
C (Δ^2)	8.38	N^{2}H′: 5.62 (3.2) N^{2}H″: 5.77 (6.3)				5.89
D (Λ^2)	8.19	N^{2}H′: 5.62 (2.3) N^{2}H″: 5.67 (1.7)				5.85
		(*R*,*S*)-**pipen**Pt(3′-GMP)$_2$				
A′ (Δ^1)	8.58	N^{1}H: 6.05 (1.9)	2.52 (2.9)		*d*	5.93
B′ (Λ^1)	8.38		2.50 (1.0)	2.81 (1.9)	*d*	5.86
C′ (Δ^2)	8.33	N^{2}H′: 5.70 (1.4) N^{2}H″: 5.74 (3.2)				5.87
D′ (Λ^2)	8.28					5.87

[a] Values in parentheses are the volumes of the cross-peaks. [b] The volume ratio is defined as the volume of the H8−C^{6}H″ cross-peak divided by the volume of the H8−NH cross-peak. [c] Δ and Λ represent the chiralities of the HT atropisomer, and the superscripts 1 and 2 denote the coordination sites cis to the secondary and the primary amine, respectively. [d] Cannot be determined due to the absence of a cross-peak.

Table 2. Chemical Shifts and Relative Volumes of NH−CH NOE Cross-Peaks for the **pipen** Moiety of (*S*,*R*)-**pipen**Pt(3′-GMP)$_2$

peak	N^{1}H	N^{2}H′	N^{2}H″	C^{1}H′	C^{1}H″	C^{2}H	C^{6}H′	C^{6}H″	rel vol
				Major Atropisomer (ΛHT)					
1	6.06			2.63					6.0
2	6.06				2.75				2.3
3	6.06					3.04			2.5
4	6.06						2.42		6.7
5	6.06							2.72	2.3
6		5.62		2.63					5.9
7		5.62			2.75				*a*
8		5.62				3.04			2.4
9			5.67	2.63					3.0
10			5.67		2.75				8.0
11			5.67			3.04			3.2
				Minor Atropisomer (ΔHT)					
12	5.71			2.67					4.7
13	5.71				2.75				1.0
14	5.71					3.08			1.6
15	5.71						2.60		8.0
16	5.71							2.88	2.0
17		5.62		2.67					2.2
18		5.62			2.75				*a*
19		5.62				3.08			3.1
20			5.77	2.67					8.0
21			5.77		2.75				5.8
22			5.77			3.08			1.0

[a] Cannot be determined due to overlap of signals.

The H8 signals have NOE cross-peaks to NH and C^{6}H signals (Table 1 and Supporting Information). For the most abundant species, peak A has a strong cross-peak with the NH signal at 6.06 ppm, while peak D has cross-peaks with NH signals at 5.67 and 5.62 ppm. This pattern demonstrates that **G$_A$** is cis to the secondary amine and **G$_D$** is cis to the primary amine. Furthermore, peak A has cross-peaks with the C^{6}H′ signal (H′ and H″ designate upper- and lower-field CH_2 signals, respectively) at 2.42 ppm and the C^{6}H″ signal at 2.72 ppm, strongly suggesting that **G$_A$** is cis to the secondary amine.

From the NOE cross-peaks between the NH and the CH_2 and CH signals of the **pipen** ligand (Table 2 and Supporting Information), the relative positions of the protons can be determined. The results are as follows: C^{6}H′ is C^{6}H$_{eq}$, C^{6}H″ is C^{6}H$_{ax}$; C^{1}H′ is C^{1}H$_{ax}$, C^{1}H″ is C^{1}H$_{eq}$; N^{2}H′ is N^{2}H$_{eq}$, N^{2}H″ is N^{2}H$_{ax}$. From these results, N^{1}H and C^{6}H″ are clearly on opposite sides of the platinum coordination plane. The ratio of the volume of the A−C^{6}H″ cross-peak to that of the A−N^{1}H cross-peak is 0.3 (Table 1), indicating that **G$_A$** H8 lies on the same side of the coordination plane as N^{1}H (Figure 3). This result shows that the most abundant atropisomer with signals A and D has the ΛHT conformation.

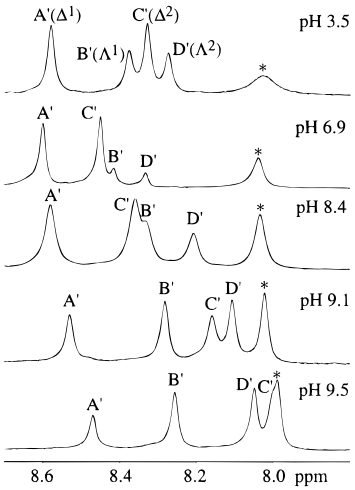

Figure 5. H8 regions of the ^{1}H NMR spectra of (*R*,*S*)-**pipen**Pt(3′-GMP)$_2$ at various pH values. The peaks labeled with an asterisk are from free 3′-GMP.

For the minor species, peak B has a cross-peak with the NH signal at 5.71 ppm, while C has cross-peaks with the NH signals at 5.62 and 5.77 ppm. This pattern demonstrates that **G$_B$** is cis to the secondary amine and **G$_C$** is cis to the primary amine. Moreover, peak B has cross-peaks with the C^{6}H′ signal at 2.60 ppm and the C^{6}H″ signal at 2.88 ppm, clearly showing that **G$_B$** H8 is cis to the secondary amine.

From the NOE cross-peaks between the NH and the CH_2 and CH signals within the **pipen** ligand (Table 2 and Supporting Information), the relative positions of the protons were determined as follows: C^{6}H′ is C^{6}H$_{eq}$, C^{6}H″ is C^{6}H$_{ax}$; C^{1}H′ is C^{1}H$_{ax}$, C^{1}H″ is C^{1}H$_{eq}$; N^{2}H′ is N^{2}H$_{ax}$, N^{2}H″ is N^{2}H$_{eq}$. The ratio of the volume of the B−C^{6}H″ cross-peak to that of the B−N^{1}H cross-peak is 18.2, indicating that **G$_B$** H8 is closer to C^{6}H″ than to N^{1}H, and therefore **G$_B$** H8 lies on the opposite side of the coordination plane from N^{1}H. Also, the C−N^{2}H′ cross-peak is smaller than the C−N^{2}H″ cross-peak, indicating that **G$_C$** H8 lies on the side of the coordination plane opposite to N^{2}H$_{ax}$. Therefore, the minor form is the ΔHT atropisomer.

(*R*,*S*)-pipenPt(3′-GMP)$_2$. In the ^{1}H NMR spectrum of (*R*,*S*)-**pipen**Pt(3′-GMP)$_2$ at pH 3.5 (Figure 5), four H8 peaks (8.8−8.0 ppm) labeled A′ to D′ comprise >90% of the H8 intensity. By integration, the areas of peaks A′ and C′ are equivalent and the areas of peaks B′ and D′ are equivalent. The ratio of the sum of the areas of A′ and C′ from the major atropisomer to that of B′ and D′ is 1.7:1. The 6.1−5.5 ppm region contains six NH signals; these have cross-peaks to the **pipen** methylene and the methine signals in the 3.1−1.0 ppm region.

The H8 signals have NOE cross-peaks to NH and C^{6}H signals (Table 1 and Supporting Information). For the most abundant species, peak A′ has a strong cross-peak with the NH signal at 6.05 ppm, while peak C′ has cross-peaks with NH signals at 5.70 and 5.74 ppm. This pattern demonstrates that **G$_{A'}$** is cis to the secondary amine and **G$_{C'}$** is cis to the primary amine. Furthermore, A′ has a cross-peak with the C^{6}H′ signal at 2.52

Table 3. Chemical Shifts and Relative Volumes of NH−CH NOE Cross-Peaks for the **pipen** Moiety of (*R,S*)-**pipen**Pt(3′-GMP)$_2$

peaks	N^1H	N^2H'	N^2H''	C^1H'	C^1H''	C^2H	C^6H'	C^6H''	rel vol
				Major Atropisomer (ΔHT)					
1	6.05			2.59					4.8
2	6.05					3.04			2.0
3	6.05						2.52		6.6
4	6.05							2.72	3.0
5		5.70		2.59					11.8
6		5.70			2.75				9.4
7		5.70				3.04			1.2
8			5.74	2.59					3.2
9			5.74		2.75				7.2
10			5.74			3.04			4.0
				Minor Atropisomer (ΛHT)					
11	5.61			2.64					4.0
12	5.61				2.72				1.2
13	5.61					3.05			1.0
14	5.61						2.50		4.2
15	5.61							2.81	1.4
16		5.52		2.64					2.2
17		5.52			2.72				2.8
18		5.52				3.05			1.8
19			5.76	2.64					4.4
20			5.76		2.72				3.2

ppm, strongly supporting the conclusion that $\mathbf{G_{A'}}$ is cis to the secondary amine.

From the NOE cross-peaks between the NH and the CH_2 and CH signals of the **pipen** ligand (Table 3 and Supporting Information), the relative positions of the protons can be determined. The relatively small NOE cross-peak between the N^1H and C^2H signals indicates that the secondary amine nitrogen and C^2 have different chiralities (Table 1). The N^1H signal has a smaller NOE cross-peak with the C^6H'' signal than with the C^6H' signal, indicating that C^6H' is C^6H_{eq}, while C^6H'' is C^6H_{ax}. The C^2H-N^2H' cross-peak is smaller than the C^2H-N^2H'' cross-peak, indicating that N^2H' is N^2H_{eq} and N^2H'' is N^2H_{ax}. Finally, the C^1H' signal has a stronger NOE cross-peak with the N^2H' signal than with the N^2H'' signal, indicating that C^1H' is C^1H_{ax}. The $C^1H''-N^2H'$ and $C^1H''-N^2H''$ NOE cross-peaks are comparable, indicating that C^1H'' is C^1H_{eq}.

From the above results, it is clear that N^1H and C^6H'' are on opposite sides of the platinum coordination plane. The orientation of the **G** bases can be deduced from the NOE cross-peaks between H8 and these proton signals. Peak A′ has a strong NOE cross-peak with N^1H but no cross-peak with C^6H_{ax} (Table 1), indicating that $\mathbf{G_{A'}}$ H8 lies on the same side of the coordination plane as N^1H. Peak C′ has a stronger NOE cross-peak to the N^2H_{ax} signal than to the N^2H_{eq} signal, indicating that $\mathbf{G_{C'}}$ H8 lies on the same side of the coordination plane as N^2H_{ax}. These results demonstrate that the most abundant species is the ΔHT atropisomer.

For the second most abundant species (Table 1), no cross-peak between H8 and NH signals can be seen. However, strong cross-peaks between peak B′ and C^6H' at 2.50 ppm and C^6H'' at 2.81 ppm indicate that $\mathbf{G_{B'}}$ is cis to the secondary amine. Therefore, $\mathbf{G_{D'}}$ must be cis to the primary amine. The relative positions of the protons in the **pipen** moiety for this atropisomer can be deduced as described above. The assignments are as follows: C^6H' is C^6H_{eq}, C^6H'' is C^6H_{ax}; C^1H' is C^1H_{ax}, C^1H'' is C^1H_{eq}; N^2H' is N^2H_{ax}, and N^2H'' is N^2H_{eq}.

Because peak B′ has a strong NOE cross-peak with the C^6H_{ax} signal and no cross-peak with the N^1H signal, $\mathbf{G_{B'}}$ H8 must lie on the opposite side of the coordination plane from N^1H. Unfortunately, since peak D′ has no cross-peak with the **pipen** moiety, its orientation cannot be determined. However, it is reasonable that this atropisomer is ΛHT since no NOE cross-peak between peaks B′ and D′ can be seen, and the orientation of $\mathbf{G_{B'}}$ is consistent with the ΛHT orientation.

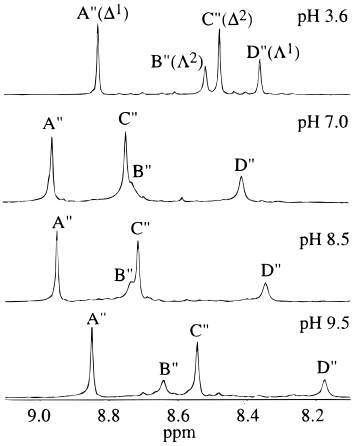

Figure 6. H8 regions of the ^1H NMR spectra of (*R,S*)-**pipen**Pt(5′-GMP)$_2$ at various pH values.

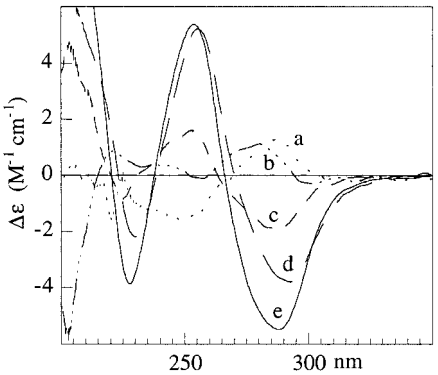

Figure 7. CD spectra of (a) [(*S,R*)-**pipen**Pt(9-EtG)$_2$]$^{2+}$ at pH 7.4 and of (b) (*S,R*)-**pipen**Pt(3′-GMP)$_2$, (c) [(*R,S*)-**pipen**Pt(9-EtG)$_2$]$^{2+}$, (d) (*R,S*)-**pipen**Pt(5′-GMP)$_2$, and (e) (*R,S*)-**pipen**Pt(3′-GMP)$_2$ at pH 3.

***(R,S)*-pipenPt(5′-GMP)$_2$.** In the ^1H NMR spectrum of (*R,S*)-**pipen**Pt(5′-GMP)$_2$ at pH 3.6, four H8 signals (8.9−8.3 ppm) labeled A″ to D″ were observed (Figure 6). By integration, the areas of peaks A″ to C″ are equivalent and the areas of peaks B″ and D′ are equivalent. The ratio of the sum of the areas of A″ and C″ from the major atropisomer to that of B″ and D″ is 1.6:1. On the basis of the CD spectrum and pH titration results discussed below, the major and minor HT isomers are the ΔHT and the ΛHT forms, respectively. $\mathbf{G_{A''}}$ and $\mathbf{G_{D''}}$ are cis to the secondary amine, and $\mathbf{G_{B''}}$ and $\mathbf{G_{C''}}$ are cis to the primary amine.

Circular Dichroism. The CD spectrum of (*S,R*)-**pipen**Pt$\mathbf{G}_2$ ($\mathbf{G}$ = 3′-GMP and 9-EtG) at pH 3 (Figure 7) shows a positive peak at about 285 nm and a negative peak at 250 nm. Spectra similar to this have been found for complexes in which ΛHT is the dominant atropisomer as determined by NMR spectroscopy;[19] therefore, this type of CD signal is designated as Λ. The CD signals of (*R,S*)-**pipen**Pt$\mathbf{G}_2$ ($\mathbf{G}$ = 3′-GMP, 5′-GMP, 9-EtG) (Figure 7) are designated as Δ since the peaks are opposite in sign to those in the CD spectra of (*S,R*)-**pipen**Pt$\mathbf{G}_2$ complexes.

pH Titration. (*S,R*)-pipenPt(3′-GMP)$_2$. NMR spectra of (*S,R*)-**pipen**Pt(3′-GMP)$_2$ at different pH values (Figure 4) indicate that, at pH 6.9, the major atropisomer has changed from the ΛHT to the ΔHT form. At pH 9.1, deprotonation of N1H occurs, and the ΛHT atropisomer becomes slightly favored as it was at low pH. The CD spectra of (*S,R*)-**pipen**Pt(3′-GMP)$_2$ between pH 7 and 9.6 (Figure 8) are consistent with the NMR

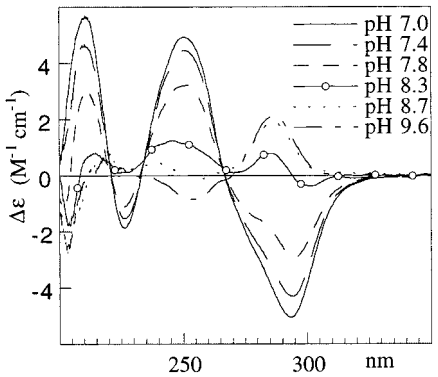

Figure 8. CD spectra of (*S*,*R*)-**pipen**Pt(3′-GMP)$_2$ at various pH values.

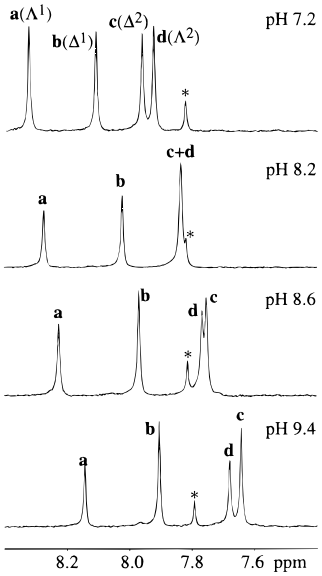

Figure 9. H8 regions of the ^{1}H NMR spectra of [(*S*,*R*)-**pipen**Pt(9-EtG)$_2$]$^{2+}$ at various pH values. The peaks labeled with an asterisk are from free 9-EtG.

results. The CD signals start to invert at about pH 8.3, consistent with a change of the dominant atropisomer at higher pH.

[(*S*,*R*)-pipenPt(9-EtG)$_2$]$^{2+}$. NMR spectra of [(*S*,*R*)-**pipen**Pt(9-EtG)$_2$]$^{2+}$ at different pH values are shown in Figure 9. At pH 7.2, four H8 signals labeled a to d have chemical shifts between 8.4 and 7.8 ppm. One of the atropisomers was slightly favored (52%). From the CD spectrum at neutral pH, this atropisomer was assigned as ΛHT. After the pH was raised, the NMR data indicate the ΔHT form became favored (62% at pH 9.4). As the pH was raised to 9.4, signals c and d shifted upfield more than their partners (Figure 9). This shift pattern suggests that $\mathbf{G_c}$ and $\mathbf{G_d}$ are cis to the primary amine (see Discussion).

(*R*,*S*)-pipenPt(3′-GMP)$_2$. The NMR spectra of (*R*,*S*)-**pipen**Pt(3′-GMP)$_2$ at different pH values (Figure 5) indicate that, at pH 6.9, the population of the ΔHT atropisomer has increased relative to pH 3. After N1H was deprotonated, the ΛHT atropisomer became the dominant species. The Δ type CD signal of (*R*,*S*)-**pipen**Pt(3′-GMP)$_2$ between pH 7.5 and 9.9 (Figure 10) decreased in intensity. However, the fact that the CD signal did not invert indicates that the ellipticity of the ΔHT form at high pH is larger than that of the ΛHT form for (*R*,*S*)-**pipen**Pt(3′-GMP)$_2$.

(*R*,*S*)-pipenPt(5′-GMP)$_2$. The NMR spectra of (*R*,*S*)-**pipen**Pt(5′-GMP)$_2$ at different pH values (Figure 6) indicate that after the phosphate group was deprotonated at pH 7.0, the major

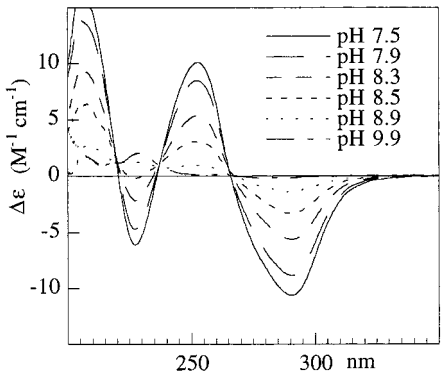

Figure 10. CD spectra of (*R*,*S*)-**pipen**Pt(3′-GMP)$_2$ at various pH values.

atropisomer was still ΔHT. At higher pH, where N1H is deprotonated, the population of the ΔHT form had increased slightly.

[(*R*,*S*)-pipenPt(9-EtG)$_2$]$^{2+}$. NMR spectra of [(*R*,*S*)-**pipen**Pt(9-EtG)$_2$]$^{2+}$ at different pH values have been obtained (data not shown). At pH 7.2, one atropisomer was slightly favored (52%). From the CD spectrum at neutral pH, this atropisomer was assigned as ΔHT. When the pH was raised, the ΛHT atropisomer was favored such that its population was 64% at pH 9.5.

Discussion

Analyzing the NOESY/EXSY data and CD results at pH ∼3.5, we found that the conformation of the favored atropisomer was Λ for all (*S*,*R*)-**pipen**Pt$\mathbf{G}_2$ complexes and Δ for all (*R*,*S*)-**pipen**Pt$\mathbf{G}_2$ complexes. Thus, the **pipen** ligand exhibited stereochemical control of the HT chirality at low pH. In general, the ratios of the population of the major HT to that of the minor HT species determined here were smaller than those found for analogous (**CCC**)Pt$\mathbf{G}_2$ complexes studied with **CCC** = C_2-symmetrical **Me$_2$DAB** or **Bip**.[2,18,19,21] The latter carrier ligands have two chiral secondary amines, and the lower stereocontrol of the **pipen** ligand is consistent with its having only one chiral amine.

The three **G**'s used in this study each have different N9 substituents. Different interactions between these substituents and the **pipen** and the cis **G** bases can exhibit a modulating influence on the atropisomer distribution. The simplest **G** derivative, 9-EtG, can form only **G** O6−NH(**pipen**) hydrogen bonds. 3′-GMP can form **G** O6−NH(**pipen**) and **G** phosphate−cis **G** hydrogen bonds. The 3′-phosphate groups can also be involved in phosphate−phosphate repulsion or electrostatic attraction to the positive charge of the Pt(II) center. 5′-GMP has potential interactions similar to those of 3′-GMP, with the added possibility of forming phosphate−NH(**pipen**) hydrogen bonds. Below, we shall explore the role of the N9 substituents by discussing our experimental results at different pH values.

pH ∼3. For [(*S*,*R*)-**pipen**Pt(9-EtG)$_2$]$^{2+}$ and [(*R*,*S*)-**pipen**Pt(9-EtG)$_2$]$^{2+}$, the percentage of the major atropisomer was 52% (Table 4). In the major HT form, an O6−NH(pip) hydrogen bond cannot form because O6 and NH(pip) are on opposite sides of the platinum coordination plane. Models suggest that the 9-Et group cannot interact well with the cis **G** base; therefore the slight preference for one HT atropisomer may just be the consequence of the modest stereochemical control exhibited by the **pipen** ligand.

For (*S*,*R*)-**pipen**Pt(5′-GMP)$_2$, the percentage of the ΛHT atropisomer was 71% (Table 4),[17] and for (*R*,*S*)-**pipen**Pt(5′-

Table 4. H8 NMR Chemical Shifts and Atropisomer Percentages of **pipen**Pt**G**$_2$ Complexes at Different pH Values

complex	pH	δ(H8), ppm Λ^1	Λ^2	Δ^1	Δ^2	% ΛHT	% ΔHT
[(*S*,*R*)-**pipen**Pt(9-EtG)$_2$]$^{2+}$	3.0	8.31	7.92	8.10	7.97	52	48
	7.2	8.33	7.92	8.11	7.96	52	48
	9.4	8.14	7.68	7.91	7.64	38	62
(*S*,*R*)-**pipen**Pt(5′-GMP)$_2$	2.9	8.67	8.35	8.37	8.48	71	30
	6.8	8.66	8.60	8.31	8.70	85	15
	10.9	8.62	8.06	8.24	8.31	28	72
(*S*,*R*)-**pipen**Pt(3′-GMP)$_2$	3.5	8.55	8.21	8.46	8.39	57	43
	6.9	8.56	8.24	8.53	8.49	34	66
	9.5	8.27	7.84	8.05	7.84	51	49
[(*R*,*S*)-**pipen**Pt(9-EtG)$_2$]$^{2+}$	3.0	8.10	7.97	8.31	7.92	48	52
	7.2	8.11	7.96	8.33	7.93	48	52
	9.5	7.90	7.63	8.13	7.67	64	36
(*R*,*S*)-**pipen**Pt(5′-GMP)$_2$	3.6	8.36	8.52	8.83	8.48	38	62
	7.0	8.41	8.73	8.97	8.75	40	60
	9.5	8.18	8.64	8.85	8.55	31	69
(*R*,*S*)-**pipen**Pt(3′-GMP)$_2$	3.5	8.38	8.27	8.58	8.33	37	63
	6.9	8.42	8.33	8.60	8.45	17	83
	9.5	8.26	8.05	8.47	7.99	65	35

GMP)$_2$, the percentage of the ΔHT atropisomer was 62% (Table 4). Against the background of results for [**pipen**Pt(9-EtG)$_2$]$^{2+}$, the 5′-phosphate group clearly further stabilizes the favored major HT atropisomer over the minor HT atropisomer. In the respective dominant ΛHT or ΔHT form of the (*S*,*R*)- and (*R*,*S*)-**pipen**Pt(5′-GMP)$_2$ complexes, the phosphate group of the **G** cis to the secondary amine is on the same side of the platinum coordination plane with respect to the cis NH. Therefore, formation of the phosphate−NH(pip) hydrogen bond appears to be a contributing factor in further stabilizing the dominant atropisomer. For (*S*,*R*)-**pipen**Pt(3′-GMP)$_2$, the percentage of the ΛHT atropisomer was 57%, and for (*R*,*S*)-**pipen**Pt(3′-GMP)$_2$, the percentage of the ΔHT atropisomer was 63% (Table 4). Formation of a 3′-phosphate−NH(**pipen**) hydrogen bond is geometrically impossible. From examination of molecular models, the 3′-phosphate group from one 3′-GMP can form intramolecular hydrogen bonds to the N1H and NH_2 groups of the cis 3′-GMP in the ΔHT conformation, whereas these hydrogen bonds are less favorable in the ΛHT conformation. Such hydrogen bonding explains the slightly greater preference for the ΔHT atropisomer in the (*R*,*S*)-**pipen** complex than in the (*S*,*R*)-**pipen** complex.

pH ∼7. For [(*S*,*R*)-**pipen**Pt(9-EtG)$_2$]$^{2+}$ and [(*R*,*S*)-**pipen**Pt-(9-EtG)$_2$]$^{2+}$, the atropisomer distribution was the same as that at pH 3 (Table 4) since no proton could be removed as the pH was raised to neutral. For (*S*,*R*)-**pipen**Pt(5′-GMP)$_2$, the population of the ΛHT atropisomer increased to 85% (Table 4); the increase is consistent with formation of stronger phosphate−NH(**pipen**) hydrogen bonding upon deprotonation of the phosphate group.[17] However, for (*R*,*S*)-**pipen**Pt(5′-GMP)$_2$, the population of the ΔHT atropisomer did not increase but actually dropped slightly to 60% (Table 4). If phosphate−NH(**pipen**) were the most important interaction, we would expect the population of the ΔHT atropisomer to increase at neutral pH. However, we find that the population of the ΛHT form of *cis*-PtA$_2$(5′-GMP)$_2$ complexes always increased after phosphate deprotonation,[3,17,21,28] independent of the nature of A$_2$. This result suggests that, in addition to phosphate−NH(**pipen**) hydrogen bonding, other interactions between cis 5′-GMP's may influence the atropisomeric distribution. For example, intramolecular hydrogen bonding between the phosphate group of one 5′-GMP and the N1H and NH_2 groups of the cis 5′-GMP may be more favorable in the ΛHT than in the ΔHT conformer. Thus, the increase in the ΛHT form of (*S*,*R*)-**pipen**Pt(5′-GMP)$_2$ reflects contributions from both types of hydrogen bonding.

For both (*S*,*R*)- and (*R*,*S*)-**pipen**Pt(3′-GMP)$_2$ complexes, the dominant species at neutral pH is ΔHT (Table 4), due to the formation of strong phosphate−cis **G** hydrogen bonds upon phosphate group deprotonation. The dominance of the ΔHT atropisomer in (*S*,*R*)- and (*R*,*S*)-**pipen**Pt(3′-GMP)$_2$ complexes is consistent with the lower stereochemical control of the **pipen** ligand; in contrast, for (**CCC**)Pt(3′-GMP)$_2$, the HT chirality of the dominant atropisomer is dependent on the chirality of the **CCC** ligand.

pH ∼10. The pK_a of the N1H group of **G** derivatives is about 9.6.[29] Platination through N7 coordination causes a drop in this pK_a by 0.46 unit for *cis*-Pt(NH$_3$)$_2$(5′-dGMP)$_2$.[29] N1H deprotonation will increase electron density on O6, making it a better hydrogen-bond acceptor. This fact has been used to explain the downfield shift of NH signals for Pt(**dien**)(5′-GMP) (**dien** = diethylenetriamine) at pH 9.[10] For (*S*,*R*)-**pipen**Pt(9-EtG)$_2$]$^{2+}$ and [(*R*,*S*)-**pipen**Pt(9-EtG)$_2$]$^{2+}$ complexes, the major conformations at pH 9.5 are ΔHT and ΛHT, respectively. In these conformations, two O6−NH(**pipen**) hydrogen bonds are possible. Therefore, O6−NH(**pipen**) hydrogen bonding is the major stabilizing interaction for [**pipen**Pt(9-EtG)$_2$]$^{2+}$ complexes at high pH.

If O6−NH(**pipen**) hydrogen bonding were the most important stabilizing force at high pH, we would expect (*S*,*R*)- and (*R*,*S*)-**pipen**Pt(3′-GMP)$_2$ to exhibit results similar to those for the respective 9-EtG adducts. However, for both (*S*,*R*)- and (*R*,*S*)-**pipen**Pt(3′-GMP)$_2$, the major conformation is ΛHT (Table 4) at high pH. Therefore, other interactions must be involved. After deprotonation of N1H, the N1 atom is negatively charged and no phosphate−N1H hydrogen bond can exist. From examination of models, the distance between the 3′-phosphate group and the N1 atom of the cis 3′-GMP is shorter in the ΔHT than in the ΛHT atropisomer. This close distance leads to favorable interaction (phosphate−N1H hydrogen bond) at pH 7 but unfavorable interaction (repulsion between negatively charged N1 and 3′-phosphate group) at high pH. Therefore, the ΔHT atropisomer is destabilized after N1H deprotonation. From examination of models again, it is obvious that the two 3′-phosphate groups are closer to each other in the ΔHT conformation. Repulsion between the negatively charged phosphate groups is greater in the ΔHT than in the ΛHT conformation. Therefore, phosphate−phosphate interaction favors the ΛHT atropisomer. Apparently, the phosphate−phosphate repulsion and the phosphate−negatively charged N1 repulsion have the effect of favoring the same atropisomer, which is the Λ form; these repulsions are collectively called cis **G** repulsions. For (*S*,*R*)-**pipen**Pt(3′-GMP)$_2$, in which O6−NH(**pipen**) hydrogen bonding favors the ΔHT atropisomer, the overall result was a small increase in the amount of the ΛHT atropisomer when the pH was raised from neutral to 9.5 (Table 4). For (*R*,*S*)-**pipen**Pt(3′-GMP)$_2$, in which both the O6−NH(**pipen**) hydrogen bonding and the cis **G** repulsions favor the ΛHT atropisomer, the result was a substantial preference for the ΛHT atropisomer at high pH (Table 4).

The major species for both (*S*,*R*)- and (*R*,*S*)-**pipen**Pt(5′-GMP)$_2$ complexes is the ΔHT atropisomer after N1H deprotonation. The explanation for this preference may be similar to that for the 3′-GMP adducts except that the cis **G** repulsions favor the ΔHT atropisomer in this case. However, since the 5′-phosphate group has greater conformational freedom than the 3′-phosphate

(28) Unpublished results from these laboratories.

(29) Song, B.; Oswald, G.; Bastian, M.; Sigel, H.; Lippert, B. *Met. Based Drugs* **1996**, *3*, 131.

group, the contributions of cis **G** repulsions are not so apparent from models.

Comparisons to CCC Analogues. Comparing the pH titration results for the **pipen** system studied here and those for the C_2-symmetrical **CCC** system,[21,28] we note some interesting observations. For (*S*,*R*)-**pipen**Pt(3′-GMP)$_2$ (Figure 4, Table 4) and (*S*,*R*,*R*,*S*)-(**CCC**)Pt(3′-GMP)$_2$ complexes,[21,28] a change in pH range from 3 to 7 increased the amount of the ΔHT atropisomer; i.e., the change of atropisomer population was in the *same* direction. As mentioned above, further increase in the pH to 9.5 increased the amount of the ΛHT atropisomer for (*S*,*R*)-**pipen**Pt(3′-GMP)$_2$ (Figure 4, Table 4). However, this pH change increased the amount of the ΔHT atropisomer for (*S*,*R*,*R*,*S*)-(**CCC**)Pt(3′-GMP)$_2$ complexes.[21,28] The change of atropisomer population was in the *opposite* direction. We believe that the explanation for this difference lies in the different hydrogen-bonding motifs of these carrier ligands. For the **pipen** system, it is possible to have two and one O6−NH(**pipen**) hydrogen bonds for the ΔHT and the ΛHT atropisomer, respectively. At high pH, conversion from the ΔHT to the ΛHT atropisomer requires accommodating the loss of only one O6−NH(**pipen**) hydrogen bond; thus, the cis **G** repulsions are the most important interactions governing the atropisomer population for the **pipen** system at high pH. For the (*S*,*R*,*R*,*S*)-(**CCC**)-Pt**G**$_2$ system,[2,18,19,21] two O6−NH(**CCC**) hydrogen bonds are possible in the ΔHT form, but no O6−NH(**CCC**) hydrogen bond is possible in the ΛHT form. Changing from the ΔHT form to the ΛHT form results in the loss of two such hydrogen bonds; thus, O6−NH(**CCC**) hydrogen bonding is the most important interaction governing the atropisomer population for the (*S*,*R*,*R*,*S*)-**CCC** systems at high pH.[28]

For the 5′-GMP complexes, (*S*,*R*)-**pipen**Pt(5′-GMP)$_2$[17] (Table 4) and (*S*,*R*,*R*,*S*)-**Me$_2$DAB**Pt(5′-GMP)$_2$,[28] the pattern of the change of atropisomer population was similar (i.e., small or no increase in the ΛHT population from pH 3 to 7 and large decreases in the ΛHT population as the pH was raised further, such that at pH 11 the dominant species was the ΔHT atropisomer in both cases). The similar result at very high pH is caused by the fact that both O6−NH hydrogen bonding and cis **G** repulsions favor the ΔHT form for the 5′-GMP adducts in these two cases. For (*S*,*R*,*R*,*S*)-**Bip**Pt(3′-GMP)$_2$, the changes in population can be explained similarly, but the ΛHT form was relatively more favored, perhaps reflecting the rigidity of the **Bip** ligand.[21]

Likewise, we can interpret the pH-dependent population changes of (*R*,*S*)-**pipen**Pt**G**$_2$ and (*R*,*S*,*S*,*R*)-(**CCC**)Pt**G**$_2$ atropisomers according to the above interactions. For both (*R*,*S*)-**pipen**Pt(3′-GMP)$_2$ (Figure 5, Table 4) and (*R*,*S*,*S*,*R*)-(**CCC**)-Pt(3′-GMP)$_2$,[28] raising the pH to 9.5 increased the amount of the ΛHT atropisomer. Again, both O6−NH hydrogen bonding and cis **G** repulsions favor the ΛHT atropisomer at high pH. For (*R*,*S*)-**pipen**Pt(5′-GMP)$_2$, conversion from the ΛHT to the ΔHT atropisomer at high pH requires accommodating the loss of only one O6−NH(**pipen**) hydrogen bond; thus, the cis **G** repulsions represent the most important interactions and favor the ΔHT atropisomer (Figure 6, Table 4). For (*R*,*S*,*S*,*R*)-(**CCC**)-Pt(5′-GMP)$_2$ complexes,[21,28] it is expected that, at high pH, the major form is ΛHT, in which two **G** O6−NH(**CCC**) hydrogen bonds can be formed. We believe that the combined cis **G** repulsions and the phosphate−NH(**CCC**) hydrogen bonds both favor the ΔHT form in the (*R*,*S*,*S*,*R*)-(**CCC**)Pt(5′-GMP)$_2$ complex. These two factors counteract the increased strength of the O6−NH(**CCC**) hydrogen bonding accompanying N1H deprotonation; thus, we observed no significant change in atropisomer population as the pH was raised to 9.5.[21,28]

Chart 2. ΔHT Atropisomers with Right-Handed and Left-Handed Tilts[a]

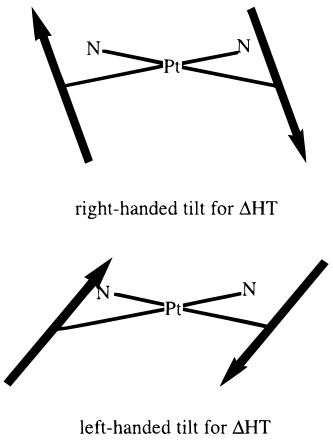

[a] The degree of the tilt is larger if the O6−NH hydrogen bond is formed.

Base Tilt and H8 Shift. In the solid state, the HT forms cluster into two groups differing in tilt;[30] i.e., the bases can have either a right-handed (R) or a left-handed (L) tilt, illustrated in Chart 2. The degrees of tilting can also be different from case to case. Relative to the average H8 signal, a lesser tilt gives less shielding and hence a deshielded H8 signal, and the greater tilt gives a shielded H8 signal. For convenience, we shall use the term "lesser tilt" even if the base plane is essentially perpendicular to the coordination plane.

We now apply this reasoning to the (*R*,*S*)-**pipen**Pt(5′-GMP)$_2$ complex studied here. All H8 signals shifted downfield as the pH was raised from 3.6 to 7.0 (Figure 6). The degree of the shift is most significant (>0.2 ppm) for **G$_B$**″ and **G$_C$**″, which are cis to the primary amine in their respective atropisomers. As the pH was further raised to 9.5, all H8 signals were shifted upfield. To explain these shift changes, we consider the ΔHT atropisomer first (Chart 3). We should note that **G$_A$**″ H8 is always distant from **G$_C$**″ (the partner of **G$_A$**″) because the phosphate−NH(**pipen**) hydrogen bond maintains a less tilted base for **G$_A$**″, regardless of any tilt changes in **G$_C$**″. Thus, **G$_A$**″ H8 is downfield throughout the pH range (Figure 6). The H8 of **G$_C$**″, on the other hand, is upfield at low pH (Figure 6) because **G$_C$**″ tilting caused by the **G$_C$**″ O6−NH(**pipen**) hydrogen bonding places **G$_C$**″ H8 close to the anisotropic **G$_A$**″ base (Chart 3). At higher pH (∼7−8), the phosphate is deprotonated and the **G$_C$**″ becomes less tilted; the greater distance of **G$_C$**″ H8 from **G$_A$**″ leads to a downfield shift (Figure 6). The **G$_A$**″ H8 signal is also shifted downfield slightly, possibly because of stronger phosphate−NH(**pipen**) hydrogen bonding. At higher pH, the **G$_C$**″ six-membered ring N1H deprotonates, probably again favoring **G$_C$**″ O6−NH(**pipen**) hydrogen bonding. The tilt change brings **G$_C$**″ H8 close to **G$_A$**″ (Chart 3), leading to the upfield shift of the **G$_C$**″ H8 signal (Figure 6).

In the ΛHT atropisomer, exactly the same sequence of tilt changes can be expected for **G$_B$**″ as described for **G$_C$**″ in the ΔHT atropisomer. However, in this case the base of the 5′-GMP cis to the secondary amine (**G$_D$**″) is always tilted toward **G$_B$**″, and the **G$_D$**″ H8 signal is always upfield (Figure 6). The above analysis for (*R*,*S*)-**pipen**Pt(5′-GMP)$_2$ is consistent with that for (*S*,*R*)-**pipen**Pt(5′-GMP)$_2$.[17]

(30) Kozelka, J.; Fouchet, M.-H.; Chottard, J.-C. *Eur. J. Biochem.* **1992**, *205*, 895.

Chart 3. The ΔHT Atropisomer of (*R,S*)-**pipen**Pt(5′-GMP)$_2$ at Different pH Values

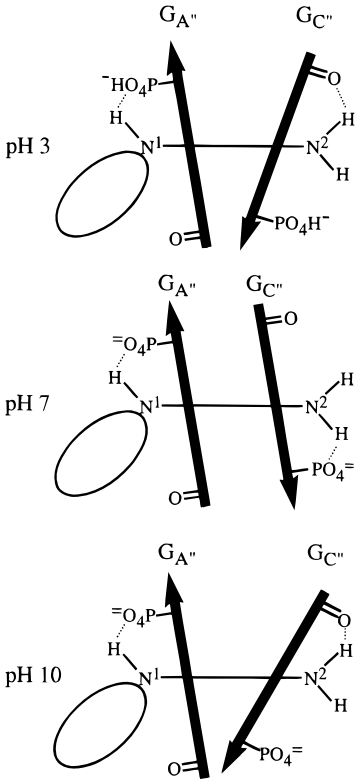

For (*R,S*)-**pipen**Pt(3′-GMP)$_2$, no interaction with NH(**pipen**) is possible for either the O6 or the phosphate group of $\mathbf{G}_{A'}$ (cis to the secondary amine in the ΔHT conformation). Therefore, $\mathbf{G}_{A'}$ has minimal tilting and the most downfield H8 NMR signal (Figure 5). $\mathbf{G}_{C'}$ is tilted toward $\mathbf{G}_{A'}$ by the $\mathbf{G}_{C'}$ O6−NH(**pipen**) hydrogen bonding; thus the $\mathbf{G}_{C'}$ H8 signal is upfield (Figure 5). As the pH is raised from 3.5 to 6.9, all H8 signals shift downfield. $\mathbf{G}_{C'}$ H8 experiences the most significant downfield shifts of all H8 signals at neutral pH (Figure 5), indicating that both bases in the ΔHT conformer are less tilted. The less tilted arrangement most probably leads to optimal phosphate−N1H hydrogen bonding and better dipole−dipole interactions. As the pH is raised above 9.0, all the H8 NMR signals shift upfield, probably because of changes in ring anisotropy upon N1H deprotonation. However, the **G** bases cis to the primary amine experience the larger shift compared to those cis to the secondary amine due to O6−NH(**pipen**) hydrogen bonding, which tilts the H8 proton toward the cis base. Note that, at pH 9.5, the $\mathbf{G}_{A'}$ and $\mathbf{G}_{C'}$ H8 signals are well separated (Figure 5), which indicates that $\mathbf{G}_{A'}$ maintains its small tilt, while $\mathbf{G}_{C'}$ adopts a large tilt accompanying **G** O6 hydrogen bonding. For (*S,R*)-**pipen**Pt(3′-GMP)$_2$, the explanation of the shift pattern is similar. Note that signals B and C are quite close and downfield at pH 6.9 (Figure 4), consistent with less tilted bases in the ΔHT form of (*S,R*)-**pipen**Pt(3′-GMP)$_2$.

Conclusions

The **pipen**Pt$\mathbf{G}_2$ complexes, by virtue of the hybrid carrier ligand, have provided insight into factors influencing preferred conformation and base tilt, into causes of the observed spectral properties, and into factors influencing the stability of the various conformers. The properties of the hybrid **pipen** ligand, with one stereocontrolling secondary amine, are intermediate between those of the complexes with more rigid and more stereocontrolling ligands and those with ammines or primary amine ligands.

Cisplatin and its analogues with achiral primary amines are anticancer active. They would not show any stereocontrol upon the HT chirality and are probably better systems than the **pipen** one for studying the secondary interactions involving the N9 substituent. Although the dynamic properties of complexes with these primary amine ligands make insightful NMR studies impossible, the results obtained here suggest that we can assess the conformations in such systems by CD methods. Such an assessment will allow us to test the hypotheses proposed[31,32] to explain the enhanced CD signals discovered two decades ago for some *cis*-Pt$A_2\mathbf{G}_2$ complexes.[24] For example, our observation of a strong Δ CD signal for *cis*-Pt$(NH_3)_2$(3′-GMP)$_2$ leaves little doubt that, in solution, this adduct adopts primarily the Δ conformation.[28] As our understanding of the factors influencing the NMR and CD spectra deepens, we may eventually be able to interpret the properties of the more dynamic adducts, even with larger molecules such as oligonucleotides.

Acknowledgment. This work was supported by NIH Grant GM 29222 (to L.G.M.), NATO CRG 950376 (to L.G.M. and G.N.), MURST (contribution 40%), the CNR, and the EC (COST Chemistry Project D8/0012/97 (to G.N.)).

Supporting Information Available: NOESY spectra of (*S,R*)-**pipen**Pt(3′-GMP)$_2$ and (*R,S*)-**pipen**Pt(3′-GMP)$_2$ and the H8 ^{1}H NMR signals of (*S,R*)-**pipen**Pt(3′-GMP)$_2$ at various pH values. This material is available free of charge on the Internet at http://pubs.acs.org.

IC981198F

(31) Gullotti, M.; Pacchioni, G.; Pasini, A.; Ugo, R. *Inorg. Chem.* **1982**, *21*, 2006.
(32) Pasini, A.; De Giacomo, L. *Inorg. Chim. Acta* **1996**, *248*, 225.